

Universal Coherence-Induced Power Losses of Quantum Heat Engines in Linear Response

Kay Brandner¹, Michael Bauer², and Udo Seifert²

¹*Department of Applied Physics, Aalto University, 00076 Aalto, Finland*

²*II. Institut für Theoretische Physik, Universität Stuttgart, 70550 Stuttgart, Germany*

We introduce a universal scheme to divide the power output of a periodically driven quantum heat engine into a classical contribution and one stemming solely from quantum coherence. Specializing to Lindblad-dynamics and small driving amplitudes, we derive general upper bounds on both, the coherent and the total power. These constraints imply that, in the linear-response regime, coherence inevitably leads to power losses. To illustrate our general analysis, we explicitly work out the experimentally relevant example of a single-qubit engine.

Heat engines are devices that convert thermal energy into useful work. A Stirling motor, for example, uses the varying pressure of a periodically heated gas to produce mechanical motion, Fig. 1a. Used by macroscopic engines for two centuries, this elementary operation principle has now been implemented on ever-smaller scales. Over the last decade, a series of experiments has shown that the working fluid of Stirling-type engines can be reduced to tiny objects such as a micrometer-seized silicon spring [1] or a single colloidal particle [2–5]. These efforts recently culminated in the realization of a single-atom heat engine [6, 7]. Thus, the dimensions of the working fluid were further decreased by four orders of magnitude within only a few years. In light of this remarkable development, the challenge of even smaller engines operating on time and energy scales comparable to Planck’s constant appears realistic for future experiments.

Such quantum engines would have access to a non-classical mechanism of energy conversion that relies on the creation of coherent superpositions between the energy levels of the working fluid [8], Fig. 1b. How does this additional freedom affect performance figures like power and efficiency? Having triggered substantial research efforts in recent years, this question constitutes one of the central problems in the emerging field of quantum thermodynamics, see for example [9–18]. However, the available results are so far inconclusive. In fact, current evidence suggests that, depending on the specific setup and benchmark parameters, coherence can, in principle, be both conducive [8, 11, 19–27] and detrimental [28–32] to the performance of thermal devices.

In this article, we universally characterize the role of coherence for the power output of cyclic heat engines in linear response. Our analysis builds on the well-established theory of open quantum systems [33, 34] and a recently developed thermodynamic framework describing periodically driven systems [30, 35], which has already proven very useful in the classical realm [36–39]. For a quantum engine, we model the working fluid as an N -level system with bare Hamiltonian H , which is embedded in a large reservoir with base temperature T [30, 40]. For simplicity, we assume that N is finite. A

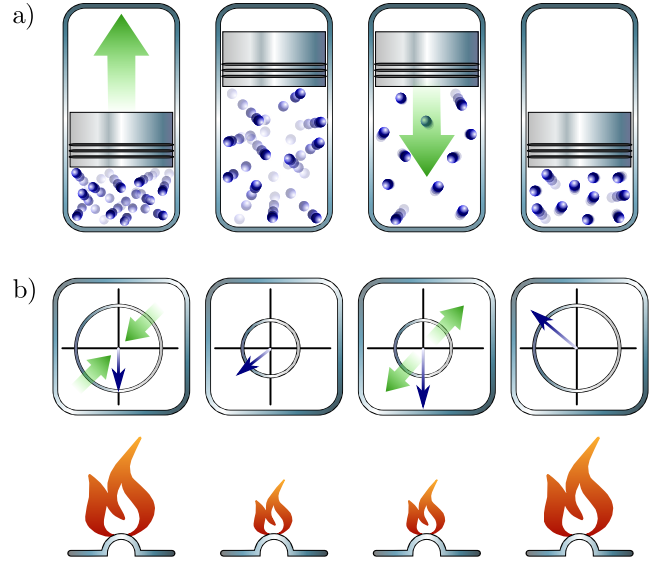


FIG. 1. Classical and quantum engines. a) Macroscopic Stirling cycle. In the first stroke, mechanical power is extracted by expanding the hot working fluid. Decreasing the temperature at constant volume in the second stroke leads to a reduction of pressure before the gas is compressed again in the third stroke. The cycle is completed by isochorically returning to the initial temperature. b) Quantum Stirling cycle. The working fluid consists of a two-level system, whose Bloch vector is shown in the four diagrams corresponding to the beginning of each stroke. Coordinates are chosen such that the instantaneous energy eigenstates lie on the vertical axis. The radius of the circle is proportional to the level splitting. Two distinct control operations are used to realize the work strokes: the level splitting is changed externally and superpositions between the two levels are created, i.e., the Bloch vector is rotated away from the vertical axis. During the thermalization strokes, coherence is irreversibly destroyed and the level population adapts to the temperature of the environment.

heat source injects thermal energy into the system by periodically heating its local environment. Hence, the working fluid effectively feels the time-dependent temperature

$$T_t \equiv T + f_t^q, \quad (1)$$

where $f_t^q \geq 0$. For work extraction, a periodic driving field f_t^w is applied, which couples linearly to the degree of freedom G_w of the system. The Hamiltonian thus acquires the time-dependence

$$H_t = H + f_t^w G^w. \quad (2)$$

For uniqueness, we assume that the field f_t^w is dimensionless and that its average over one period \mathcal{T} vanishes.

This engine delivers the mean power output

$$P = -\frac{1}{\mathcal{T}} \int_0^{\mathcal{T}} dt \operatorname{tr}\{\dot{H}_t \varrho_t\}, \quad (3)$$

where ϱ_t denotes the periodic state of the system [33]. Using the spectral decomposition

$$H_t \equiv \sum_n E_t^n |n_t\rangle \langle n_t| \quad (4)$$

of the time-dependent Hamiltonian, P can be divided into two contributions corresponding to the different mechanisms of work extraction illustrated in Fig. 1. First, the classical power

$$P^d \equiv -\frac{1}{\mathcal{T}} \int_0^{\mathcal{T}} dt \sum_n \dot{E}_t^n \langle n_t | \varrho_t | n_t \rangle \quad (5)$$

is generated by changing the energy levels of the working fluid, i.e., the diagonal elements of its Hamiltonian with respect to the unperturbed energy eigenstates. Second, the coherent power

$$P^c \equiv P - P^d = \frac{1}{\mathcal{T}} \int_0^{\mathcal{T}} dt \sum_n \langle \dot{n}_t | [H_t, \varrho_t] | n_t \rangle \quad (6)$$

arises from creating superpositions between the instantaneous energy eigenstates [41]. Accordingly, P^c vanishes when ϱ_t commutes with H_t throughout one operation cycle. This condition is met, for example, in the adiabatic limit, where the state of the system follows the instantaneous Boltzmann distribution.

For deriving constraints on the coherent power P^c , we have to specify the dissipative dynamics of the working fluid. To this end, we invoke the standard condition of weak coupling between system and reservoir. In equilibrium, i.e., for $f_t^q = f_t^w = 0$, the state ϱ_t evolves according to the Markovian master equation [34]

$$\partial_t \varrho_t = -\frac{i}{\hbar} [H, \varrho_t] + \mathcal{D} \varrho_t, \quad (7)$$

where the dissipator

$$\mathcal{D}X \equiv \sum_{\sigma} \frac{\gamma_{\sigma}}{2} ([V_{\sigma} X, V_{\sigma}^{\dagger}] + [V_{\sigma}, X V_{\sigma}^{\dagger}]) \quad (8)$$

accounts for the influence of the thermal environment [42]. Furthermore, \hbar denotes Planck's constant and $\{\gamma_{\sigma}\}$ is a set of positive rates with corresponding Lindblad operators $\{V_{\sigma}\}$. Due to microreversibility, these quantities

are constrained by the quantum detailed balance relation, which can be expressed compactly in terms of the formal identity [42, 43]

$$\mathcal{D} e^{-\beta H} = e^{-\beta H} \mathcal{D}^{\dagger}. \quad (9)$$

Here, $\beta \equiv 1/(k_B T)$, k_B denotes Boltzmann's constant and the adjoint dissipator is given by

$$\mathcal{D}^{\dagger} X \equiv \sum_{\sigma} \frac{\gamma_{\sigma}}{2} (V_{\sigma}^{\dagger} [X, V_{\sigma}] + [V_{\sigma}^{\dagger}, X] V_{\sigma}). \quad (10)$$

Provided that the cycle period \mathcal{T} is large compared to the relaxation time of the reservoir, finite driving can be included in this framework by allowing the rates and Lindblad operators to be time-dependent and replacing H and T with H_t and T_t respectively in (7)-(10) [33]. Solving the master equation (7) by treating f_t^q and f_t^w as first-order perturbations then yields the explicit expressions [44]

$$\begin{aligned} P^d &\equiv -\frac{1}{\mathcal{T}} \int_0^{\mathcal{T}} dt \int_0^{\infty} d\tau \dot{f}_t^w (\dot{C}_{\tau}^{\text{dd}} f_{t-\tau}^w + \dot{C}_{\tau}^{\text{dq}} f_{t-\tau}^q) \quad \text{and} \\ P^c &\equiv -\frac{1}{\mathcal{T}} \int_0^{\mathcal{T}} dt \int_0^{\infty} d\tau \dot{f}_t^w \dot{C}_{\tau}^{\text{cc}} f_{t-\tau}^w \end{aligned} \quad (11)$$

for the classical and the coherent power, respectively [45], in the following notation. We abbreviate with C_t^{ab} the Kubo correlation function [46]

$$C_t^{ab} \equiv \langle\langle \hat{G}_t^a, \hat{G}_0^b \rangle\rangle \equiv \int_0^{\beta} d\lambda (\langle \hat{G}_t^a e^{-\lambda H} \hat{G}_0^b e^{\lambda H} \rangle - \langle \hat{G}_t^a \rangle \langle \hat{G}_0^b \rangle), \quad (12)$$

where $t \geq 0$, $a, b = d, c, q$. Hats indicate Heisenberg-picture operators satisfying the adjoint master equation

$$\partial_t \hat{X}_t = \frac{i}{\hbar} [H, \hat{X}_t] + \mathcal{D}^{\dagger} \hat{X}_t \quad (13)$$

with initial condition $\hat{X}_0 = X$ [34]. The angular brackets in (12) denote the thermal average, i.e.,

$$\langle X \rangle \equiv \operatorname{tr}\{X e^{-\beta H}\} / \operatorname{tr}\{e^{-\beta H}\}. \quad (14)$$

Finally, we have defined the operator $G^q \equiv -H/T$ and split the control variable G^w into a diagonal, quasi-classical, and a coherent part,

$$G^d \equiv \sum_n |n\rangle \langle n| G^w |n\rangle \langle n| \quad \text{and} \quad G^c \equiv G^w - G^d, \quad (15)$$

where the vectors $|n\rangle$ correspond to the eigenstates of the unperturbed Hamiltonian H .

As a first key-observation, we note that the expression (11) for P^c is independent of the temperature profile f_t^q . Thus, under linear-response conditions, it is impossible to convert thermal energy provided by the heat source into positive power output via quantum coherence; rather coherent power can only be injected into the

system through mechanical driving. This constraint is captured quantitatively by the bound

$$P^c \leq -\frac{L_1^c \Omega^2}{\Omega^2 + L_2^c/L_1^c} F^w \leq 0, \quad (16)$$

which is saturated in the two limits $\Omega \rightarrow 0$ and $\Omega \rightarrow \infty$, for the proof see [47]. Besides the cycle frequency $\Omega \equiv 2\pi/\mathcal{T}$, the bound (16) involves the mean square amplitude

$$F^w \equiv \frac{1}{\mathcal{T}} \int_0^{\mathcal{T}} dt (f_t^w)^2 \quad (17)$$

of the driving field, and the Green-Kubo type coefficients

$$L_j^c \equiv \int_0^{\infty} dt \langle \hat{G}_t^{c(j)}, \hat{G}_0^{c(j)} \rangle \geq 0, \quad (18)$$

where the index j in brackets means a time-derivative of respective order.

The bound (16) can be understood intuitively by identifying the parameter L_2^c/L_1^c as an estimator for the decoherence strength of the reservoir, i.e., the square of the mean rate, at which its influence destroys coherent superpositions between the energy levels of the working fluid. In the incoherent limit $L_2^c/L_1^c \gg \Omega^2$, the coherent power can approach zero due to frequent interactions with the environment constantly forcing the system into a state that is diagonal in the instantaneous energy eigenbasis. This behavior resembles the quantum Zeno effect with the role of the observer played by the thermal reservoir [34]. If $L_2^c/L_1^c \ll \Omega^2$, the bath-induced decoherence is slow compared to the external driving. In this limit, coherences can be fully established such that maximal coherent power is injected into the system. Accordingly, the upper bound (16) reduces to $P^c \leq -L_1^c F^w$, its minimum with respect to Ω .

The coefficients (18) vanish if and only if $G^c = 0$, which means that the control variable G^w commutes with the unperturbed Hamiltonian H . Thus, according to (16), any non-classical driving will inevitably reduce the net output $P = P^d + P^c$ of the engine. In fact, P is subject to the upper bound

$$P \leq \frac{L_1^q F^q}{4(1 + \psi_\Omega)}, \quad \text{where } \psi_\Omega \equiv \frac{(L_1^c/L_1^d)\Omega^2}{\Omega^2 + L_2^c/L_1^c} \geq 0 \quad (19)$$

provides a measure for the relative strength of coherent and classical driving and

$$F^q \equiv \frac{1}{\mathcal{T}} \int_0^{\mathcal{T}} dt (f_t^q - \bar{f}^q)^2 \quad \text{with} \quad \bar{f}^q \equiv \frac{1}{\mathcal{T}} \int_0^{\mathcal{T}} dt f_t^q \quad (20)$$

corresponds to the mean square magnitude of the local temperature variation induced by the heat source. This bound is proven in [47]. As the bound (16), it involves a set of protocol-independent parameters L_j^a , which are reminiscent of linear transport coefficients. For $a = d$ and $a = q$, these quantities are defined analogously to (18) with G^c replaced by G^d and G^q , respectively.

In the special case of purely coherent driving, $G^d = 0$, the coefficient L_1^d vanishes. The coherence parameter ψ_Ω then diverges and (19) reduces to $P \leq 0$. Consequently in line with our analysis above, no cyclic engine relying only on coherent work extraction can properly operate in the linear-response regime. For $G^c = 0$, i.e., quasi-classical driving, ψ_Ω vanishes and the constraint (19) assumes its weakest form

$$P \leq L_1^q F^q/4. \quad (21)$$

This bound can be saturated if and only if

$$G^w = -\mu H/T \quad \text{and} \quad D^\dagger H = -\lambda(H - \langle H \rangle) \quad (22)$$

for some real scalars μ and $\lambda > 0$, see [47]. Thus, the control field f_t^w has to couple directly to the free Hamiltonian H , and the energy correlation function must decay exponentially with rate λ , i.e.,

$$\langle \hat{H}_t, \hat{H}_0 \rangle = e^{-\lambda t} \langle \hat{H}_0, \hat{H}_0 \rangle. \quad (23)$$

If these two requirements are fulfilled, as we show in [47], the protocol for optimal power extraction is determined by the condition

$$2\dot{f}_t^w = \lambda(f_t^q - \bar{f}^q)/\mu - \dot{f}_t^q/\mu, \quad (24)$$

which leads to $P = L_1^q F^q/4$ for any temperature profile f_t^q and sufficiently short operation cycles [48]. Furthermore, using relation (23), the upper bound (21) can be expressed in a physically transparent way. Specifically, we obtain

$$\frac{L_1^q F^q}{4} = \lambda \frac{\langle H^2 \rangle - \langle H \rangle^2}{4k_B T^3} F^q \quad (25)$$

by evaluating (18). Hence, the strength and the decay rate of the energy fluctuations in equilibrium essentially determine the maximum power output of a cyclic N -level engine in the linear-response regime. A similar result was obtained only recently for classical machines obeying Fokker-Planck type dynamics [35, 37].

We will now explore the quality of our general bounds under practical conditions. To this end, we consider a two-level engine with time-dependent Hamiltonian

$$H_t = \frac{\hbar\omega}{2} \sigma_z + \frac{\hbar\omega f_t^w}{2} (r\sigma_z + (1-r)\sigma_x). \quad (26)$$

Here, $\sigma_{x,y,z}$ are the usual Pauli matrices and the dimensionless parameter $0 \leq r \leq 1$ determines the relative weight of the classical and the coherent parts, $G^d = r(\hbar\omega/2)\sigma_z$ and $G^c = (1-r)(\hbar\omega/2)\sigma_x$, of the control variable G^w . The corresponding equilibrium dissipator (8) involves two Lindblad operators, $V_\pm = (\sigma_x \pm i\sigma_y)/2$, acting at the rates $\gamma_\pm \equiv \gamma e^{\mp\kappa}$, respectively, where $\kappa \equiv \hbar\omega\beta/2$. This setup lies within the range of forthcoming experiments using a superconducting qubit to realize the system and ultra fast electron thermometers for calorimetric

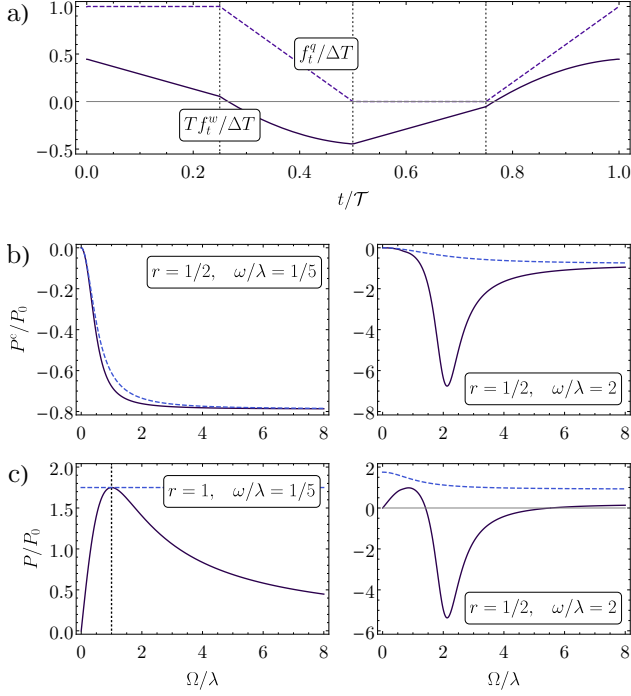


FIG. 2. Results for the single-qubit engine. a) The temperature profile f_t^q (dashed line) consists of two isothermal steps corresponding to the net temperatures $T + \Delta T$ and T , which are connected by linear slopes. The work protocol f_t^w (solid line) is determined by the condition (28). b) Coherent power (solid line) in units of $P_0 \equiv (\hbar\omega\lambda/2)(\Delta T/T)^2 10^{-2}$ as a function of the rescaled cycle frequency Ω/λ . The bound (27) is shown for comparison (dashed line). c) Plots of the total power (solid line) and its upper bound (27) (dashed line). For all parts of this figure, we have set $\kappa \equiv 1$. Symbols are explained in the main text.

work measurements [49–51]. Its coherent and total power are subject to the bounds

$$P^c \leq -\frac{\hbar\omega\lambda}{2} r^2 g \psi_\Omega F^w \quad \text{and} \quad P \leq \frac{\hbar\omega\lambda}{8} \frac{g}{1 + \psi_\Omega} \frac{F^q}{T^2}$$

$$\text{with} \quad \psi_\Omega = \frac{(1-r)^2}{r^2} \frac{\sinh 2\kappa}{4\kappa} \frac{\Omega^2}{\Omega^2 + \omega^2 + \lambda^2/4}, \quad (27)$$

$g \equiv \kappa / \cosh^2 \kappa$ and $\lambda \equiv 2\gamma \cosh \kappa$, which follow from (16) and (19) upon evaluation of the coefficients (18), see [47].

To assess the quality of these constraints, we choose a temperature profile f_t^q that mimics the Stirling cycle illustrated in Fig. 1 and a work protocol satisfying

$$2\dot{f}_t^w = -\Omega(f_t^q - \bar{f}^q)/T + \dot{f}_t^q/T, \quad (28)$$

both shown in Fig. 2a. This choice renders the amplitude and shape of f_t^w independent of the cycle frequency Ω . In Fig. 2b, the resulting coherent power is plotted as a function of Ω/λ for $r = 1/2$. If the level splitting ω is significantly smaller than the dissipation rate λ , it decays monotonically while closely following its upper

bound (27). With increasing ω , a resonant dip emerges close to $\Omega = \omega$. This feature is not reproduced by our bound, which is, however, still saturated in the limits $\Omega/\lambda \rightarrow 0$ and $\Omega/\lambda \rightarrow \infty$. For $r = 1$, the coherent power vanishes and the two conditions (22) are fulfilled with $\mu = -T$. The total power P plotted in Fig. 2c then reaches its upper bound (27) at $\Omega = \lambda$, i.e., when the work protocol (28) satisfies the maximum-power condition (24). As r varies from 1 to 0, the total power decreases more and more due to coherence-induced losses and the bound (27) lies well above the actual value of P for any cycle frequency. This result underlines our general conclusion that coherence has a purely detrimental effect on power in the linear-response regime.

For a perspective beyond linear response, we stress that our key expressions (5) and (6) are valid for arbitrarily strong driving and any thermodynamically consistent time-evolution of the working fluid. The coherent power (6) thus constitutes a universal indicator for the impact of quantum effects on thermal power generation. It can therefore be used as a unifying performance benchmark across various different types of cyclic quantum machines. In particular, it would be applicable to rapidly driven [25, 52–56] and strongly coupled [57–61] engines, which are currently subject to active investigations. Furthermore, the general framework introduced in this article could lead to a new perspective on a phenomenon earlier interpreted as a quantum analogue of classical friction, which was observed in models describing the working fluid as an interacting spin system [28, 29, 62–64].

As one of the earliest quantum heat engines, the three-level maser relies solely on non-classical work extraction [65, 66]. This example, which does not admit a linear-response description [30], shows that the coherent power can indeed become positive if the driving is strong. Coupled to two reservoirs with time-independent temperature, the three-level maser works in a steady state with respect to a rotating basis of its Hilbert space. This operation principle is similar to the one used by thermoelectric nano devices, where a spatial temperature gradient drives an electric current [67]. Extending the concept of coherent power to this second class of quantum engines, which has recently attracted remarkable interest [68–79] represents a challenge promising to reveal rich and interesting physics. Eventually, our approach could lead to a comprehensive understanding of the role of quantum effects for one of the most fundamental thermodynamic operations: the conversion of heat into power.

Acknowledgments: KB acknowledges financial support from the Academy of Finland (Contract No. 296073) and is affiliated with the Centre of Quantum Engineering. KB thanks J.P. Pekola, M. Campisi and R. Fazio for insightful discussions.

-
- [1] P. G. Steeneken, K. Le Phan, M. J. Goossens, G. E. J. Koops, G. J. A. M. Brom, C. van der Avoort, and J. T. M. van Beek, “Piezoresistive heat engine and refrigerator,” *Nature Phys.* **7**, 354 (2010).
- [2] V. Blickle and C. Bechinger, “Realization of a micrometer-sized stochastic heat engine,” *Nature Phys.* **8**, 143 (2011).
- [3] I. A. Martínez, É. Roldán, L. Dinis, D. Petrov, and R. A. Rica, “Adiabatic Processes Realized with a Trapped Brownian Particle,” *Phys. Rev. Lett.* **114**, 120601 (2015).
- [4] I. A. Martínez, É. Roldán, L. Dinis, D. Petrov, J. M. R. Parrondo, and R. A. Rica, “Brownian Carnot engine,” *Nature Phys.* **12**, 67 (2015).
- [5] S. Krishnamurthy, S. Ghosh, D. Chatterji, R. Ganapathy, and A. K. Sood, “A micrometer-sized heat engine operating between bacterial reservoirs,” *Nature Phys.* **12**, 1134 (2016).
- [6] J. Roßnagel, S. T. Dawkins, K. N. Tolazzi, O. Abah, E. Lutz, F. Schmidt-Kaler, and K. Singer, “A single-atom heat engine,” *Science* **352**, 325 (2015).
- [7] O. Abah, J. Roßnagel, G. Jacob, S. Deffner, F. Schmidt-Kaler, K. Singer, and E. Lutz, “Single-Ion Heat Engine at Maximum Power,” *Phys. Rev. Lett.* **109**, 203006 (2012).
- [8] R. Uzdin, A. Levy, and R. Kosloff, “Equivalence of Quantum Heat Machines, and Quantum-Thermodynamic Signatures,” *Phys. Rev. X* **5**, 031044 (2015).
- [9] H. T. Quan, Yu-xi Liu, C. P. Sun, and F. Nori, “Quantum Thermodynamic Cycles and quantum heat engines,” *Phys. Rev. E* **76**, 031105 (2007).
- [10] K. Funo, Y. Watanabe, and M. Ueda, “Thermodynamic work gain from entanglement,” *Phys. Rev. A* **88**, 052319 (2013).
- [11] J. Roßnagel, O. Abah, F. Schmidt-Kaler, K. Singer, and E. Lutz, “Nanoscale Heat Engine Beyond the Carnot Limit,” *Phys. Rev. Lett.* **112**, 030602 (2014).
- [12] J. P. Pekola, “Towards quantum thermodynamics in electronic circuits,” *Nature Phys.* **11**, 118 (2015).
- [13] H. Zhou, J. Thingna, P. Hänggi, J.-S. Wang, and B. Li, “Boosting thermoelectric efficiency using time-dependent control,” *Sci. Rep.* **5**, 14870 (2015).
- [14] M. Lostaglio, K. Korzekwa, D. Jennings, and T. Rudolph, “Quantum Coherence, Time-Translation Symmetry, and Thermodynamics,” *Phys. Rev. X* **5**, 021001 (2015).
- [15] P. Ćwikliński, M. Studziński, M. Horodecki, and J. Oppenheim, “Limitations on the Evolution of Quantum Coherences: Towards Fully Quantum Second Laws of Thermodynamics,” *Phys. Rev. Lett.* **115**, 210403 (2015).
- [16] B. Gardas and S. Deffner, “Thermodynamic universality of quantum Carnot engines,” *Phys. Rev. E* **92**, 042126 (2015).
- [17] H. Tasaki, “Quantum Statistical Mechanical Derivation of the Second Law of Thermodynamics: A Hybrid Setting Approach,” *Phys. Rev. Lett.* **116**, 170402 (2016).
- [18] J. Jaramillo, M. Beau, and A. Del Campo, “Quantum supremacy of many-particle thermal machines,” *New J. Phys.* **18**, 075019 (2016).
- [19] M. O. Scully, K. R. Chapin, K. E. Dorfman, M. B. Kim, and A. Svidzinsky, “Quantum heat engine power can be increased by noise-induced coherence,” *Proc. Natl. Acad. Sci. USA* **108**, 15097 (2011).
- [20] S. Abe and S. Okuyama, “Role of the superposition principle for enhancing the efficiency of the quantum-mechanical Carnot engine,” *Phys. Rev. E* **85**, 011104 (2012).
- [21] L. A. Correa, J. P. Palao, D. Alonso, and G. Adesso, “Quantum-enhanced absorption refrigerators,” *Sci. Rep.* **4**, 3949 (2014).
- [22] J. M. Horowitz and K. Jacobs, “Quantum effects improve the energy efficiency of feedback control,” *Phys. Rev. E* **89**, 042134 (2014).
- [23] K. Brandner, M. Bauer, M. T. Schmid, and U. Seifert, “Coherence-enhanced efficiency of feedback-driven quantum engines,” *New J. Phys.* **17**, 065006 (2015).
- [24] M. T. Mitchison, M. P. Woods, J. Prior, and M. Huber, “Coherence-assisted single-shot cooling by quantum absorption refrigerators,” *New J. Phys.* **17**, 115013 (2015).
- [25] D. Gelbwaser-Klimovsky, W. Niedenzu, P. Brumer, and G. Kurizki, “Power enhancement of heat engines via correlated thermalization in a three-level working fluid,” *Sci. Rep.* **5**, 14413 (2015).
- [26] R. Uzdin, “Coherence-Induced Reversibility and Collective Operation of Quantum Heat Machines via Coherence Recycling,” *Phys. Rev. Appl.* **6**, 024004 (2016).
- [27] G. Watanabe, B. P. Venkatesh, P. Talkner, and A. del Campo, “Quantum Performance of Thermal Machines Over Many Cycles,” *Phys. Rev. Lett.* **118**, 050601 (2017).
- [28] T. Feldmann and R. Kosloff, “Quantum four-stroke heat engine: Thermodynamic observables in a model with intrinsic friction,” *Phys. Rev. E* **68**, 016101 (2003).
- [29] T. Feldmann and R. Kosloff, “Characteristics of the limit cycle of a reciprocating quantum heat engine,” *Phys. Rev. E* **70**, 046110 (2004).
- [30] K. Brandner and U. Seifert, “Periodic thermodynamics of open quantum systems,” *Phys. Rev. E* **93**, 062134 (2016).
- [31] A. Roulet, S. Nimmrichter, J. M. Arrazola, and V. Scarani, “Autonomous Rotor Heat Engine,” (2016), [arXiv:1609.06011](https://arxiv.org/abs/1609.06011).
- [32] B. Karimi and J. P. Pekola, “Otto refrigerator based on a superconducting qubit - classical and quantum performance,” *Phys. Rev. B* **94**, 184503 (2016).
- [33] R. Alicki, “The quantum open system as a model of the heat engine,” *J. Phys. A: Math. Gen.* **12**, L103 (1979).
- [34] H.-P. Breuer and F. Petruccione, *The Theory of Open Quantum Systems*, 1st ed. (Clarendon Press, Oxford, 2006).
- [35] K. Brandner, K. Saito, and U. Seifert, “Thermodynamics of Micro- and Nano-Systems Driven by Periodic Temperature Variations,” *Phys. Rev. X* **5**, 031019 (2015).
- [36] K. Proesmans and C. Van den Broeck, “Onsager Coefficients in Periodically Driven Systems,” *Phys. Rev. Lett.* **115**, 090601 (2015).
- [37] M. Bauer, K. Brandner, and U. Seifert, “Optimal performance of periodically driven, stochastic heat engines under limited control,” *Phys. Rev. E* **93**, 042112 (2016).
- [38] K. Proesmans, Y. Dreher, M. Gavrilov, J. Bechhoefer, and C. Van den Broeck, “Brownian Duet: A Novel Tale of Thermodynamic Efficiency,” *Phys. Rev. X* **6**, 041010 (2016).
- [39] K. Proesmans, B. Cleuren, and C. Van den Broeck, “Power-Efficiency-Dissipation Relations in Linear Thermodynamics,” *Phys. Rev. Lett.* **116**, 220601 (2016).

- [40] R. Kosloff, “Quantum Thermodynamics: A Dynamical Viewpoint,” *Entropy* **15**, 2100 (2013).
- [41] To make these definitions unique, we understand that the time-dependent energy eigenvalues are arranged in increasing order, i.e., $E_t^0 \leq E_t^1 \leq \dots \leq E_t^N$ for any $t \in \mathbb{R}$. Furthermore, we note that the expressions (5) and (6) are unaltered if the instantaneous energy eigenstates are multiplied with arbitrary time-dependent phase factors.
- [42] H. Spohn and J. L. Lebowitz, “Irreversible thermodynamics for quantum systems weakly coupled to thermal reservoirs,” *Adv. Chem. Phys.* **38**, 109 (1978).
- [43] R. Alicki, “On the detailed balance condition for non-Hamiltonian systems,” *Rep. Math. Phys.* **10**, 249 (1976).
- [44] To obtain (11) from (5) and (6), standard linear-response theory is applied. This derivation exploits that, due to the detailed balance relation (9), the space of all system operators commuting with the unperturbed Hamiltonian H is invariant under the action of the super operators D and D^\dagger , for details see [30].
- [45] The detailed-balance relation (9) implies that the set of Lindblad operators $\{V_\alpha\}$ is self-adjoint [43, 80]. Additionally, we here assume that this set is irreducible such that $X = 1$ is the only solution of $D^\dagger X = 0$ [81]. Under this condition, the improper integrals showing up in (11) are well-defined [30].
- [46] R. Kubo, M. Toda, and N. Hashitsume, *Statistical Physics II - Nonequilibrium Statistical Mechanics*, 2nd ed. (Springer, Tokyo, 1998).
- [47] “Supplemental Material at URL,” .
- [48] For long cycles, the reduced temperature profile $f_t^q - \bar{f}^q$ would oscillate slowly and thus be either positive or negative over substantial time ranges. Consequently, integrating (24) would yield a driving protocol f_t^w with large amplitude, which violates the linear-response condition underlying the derivations leading to (21) and (24).
- [49] S. Gasparinetti, K. L. Viisanen, O.-P. Saira, T. Faivre, M. Arzeo, M. Meschke, and J. P. Pekola, “Fast Electron Thermometry for Ultrasensitive Calorimetric Detection,” *Phys. Rev. Appl.* **3**, 014007 (2015).
- [50] K. L. Viisanen, S. Suomela, S. Gasparinetti, O.-P. Saira, J. Ankerhold, and J. P. Pekola, “Incomplete measurement of work in a dissipative two level system,” *New J. Phys.* **17**, 055014 (2015).
- [51] J. P. Pekola, P. Solinas, A. Shnirman, and D. V. Averin, “Calorimetric measurement of work in a quantum system,” *New J. Phys.* **15**, 115006 (2013).
- [52] G. B. Cuetara, A. Engel, and M. Esposito, “Stochastic thermodynamics of rapidly driven systems,” *New J. Phys.* **17**, 055002 (2015).
- [53] R. Alicki and D. Gelbwaser-Klimovsky, “Non-equilibrium quantum heat machines,” *New J. Phys.* **17**, 115012 (2015).
- [54] D. Gelbwaser-Klimovsky and G. Kurizki, “Heat-machine control by quantum-state preparation: From quantum engines to refrigerators,” *Phys. Rev. E* **90**, 022102 (2014).
- [55] D. Gelbwaser-Klimovsky, R. Alicki, and G. Kurizki, “Minimal universal quantum heat machine,” *Phys. Rev. E* **87**, 012140 (2013).
- [56] M. Kolář, D. Gelbwaser-Klimovsky, R. Alicki, and G. Kurizki, “Quantum Bath Refrigeration towards Absolute Zero: Challenging the Unattainability Principle,” *Phys. Rev. Lett.* **109**, 090601 (2012).
- [57] M. Esposito, M. A. Ochoa, and M. Galperin, “Nature of heat in strongly coupled open quantum systems,” *Phys. Rev. B* **92**, 235440 (2015).
- [58] R. Uzdin, A. Levy, and R. Kosloff, “Quantum heat machines equivalence, work extraction beyond markovianity, and strong coupling via heat exchangers,” *Entropy* **18**, 124 (2016).
- [59] P. Strasberg, G. Schaller, N. Lambert, and T. Brandes, “Nonequilibrium thermodynamics in the strong coupling and non-Markovian regime based on a reaction coordinate mapping,” *New J. Phys.* **18**, 073007 (2016).
- [60] M. Carrega, P. Solinas, M. Sassetti, and U. Weiss, “Energy Exchange in Driven Open Quantum Systems at Strong Coupling,” *Phys. Rev. Lett.* **116**, 240403 (2016).
- [61] D. Newman, F. Mintert, and A. Nazir, “Performance of a quantum heat engine at strong reservoir coupling,” (2016), arXiv:1609.04035.
- [62] T. Feldmann and R. Kosloff, “Short time cycles of purely quantum refrigerators,” *Phys. Rev. E* **85**, 051114 (2012).
- [63] T. Feldmann and R. Kosloff, “Quantum lubrication: Suppression of friction in a first-principles four-stroke heat engine,” *Phys. Rev. E* **73**, 025107(R) (2006).
- [64] R. Kosloff and T. Feldmann, “Discrete four-stroke quantum heat engine exploring the origin of friction,” *Phys. Rev. E* **65**, 055102(R) (2002).
- [65] E. Geva and R. Kosloff, “Three-level quantum amplifier as a heat engine: A study in finite-time thermodynamics,” *Phys. Rev. E* **49**, 3903 (1994).
- [66] H. E. D. Scovil and E. O. Schulz-DuBois, “Three Level Masers as Heat Engines,” *Phys. Rev. Lett.* **2**, 262 (1959).
- [67] T. E. Humphrey and H. Linke, “Quantum, cyclic, and particle-exchange heat engines,” *Physica E* **29**, 390 (2005).
- [68] K. Brandner, K. Saito, and U. Seifert, “Strong Bounds on Onsager Coefficients and Efficiency for Three-Terminal Thermoelectric Transport in a Magnetic Field,” *Phys. Rev. Lett.* **110**, 070603 (2013).
- [69] K. Brandner and U. Seifert, “Multi-terminal thermoelectric transport in a magnetic field: Bounds on Onsager coefficients and efficiency,” *New J. Phys.* **15**, 105003 (2013).
- [70] D. Venturelli, R. Fazio, and V. Giovannetti, “Minimal Self-Contained Quantum Refrigeration Machine Based on Four Quantum Dots,” *Phys. Rev. Lett.* **110**, 256801 (2013).
- [71] R. S. Whitney, “Most Efficient Quantum Thermoelectric at Finite Power Output,” *Phys. Rev. Lett.* **112**, 130601 (2014).
- [72] J. Matthews, F. Battista, D. Sánchez, P. Samuelsson, and H. Linke, “Experimental verification of reciprocity relations in quantum thermoelectric transport,” *Phys. Rev. B* **90**, 165428 (2014).
- [73] C. Bergenfeldt, P. Samuelsson, B. Sothmann, C. Flindt, and M. Büttiker, “Hybrid Microwave-Cavity Heat Engine,” *Phys. Rev. Lett.* **112**, 076803 (2014).
- [74] P. P. Hofer, J. R. Souquet, and A. A. Clerk, “Quantum heat engine based on photon-assisted Cooper pair tunneling,” *Phys. Rev. B* **93**, 041418(R) (2016).
- [75] R. Sánchez, B. Sothmann, and A. N. Jordan, “Chiral Thermoelectrics with Quantum Hall Edge States,” *Phys. Rev. Lett.* **114**, 146801 (2015).
- [76] K. Brandner and U. Seifert, “Bound on thermoelectric power in a magnetic field within linear response,” *Phys. Rev. E* **91**, 012121 (2015).
- [77] G. Marchegiani, P. Virtanen, F. Giazotto, and M. Campisi, “Self-Oscillating Josephson Quantum Heat Engine,” *Phys. Rev. Appl.* **6**, 054014 (2016).

- [78] P. Samuelsson, S. Kheradsoud, and B. Sothmann, “Optimal quantum interference thermoelectric heat engine with edge states,” (2016), [arXiv:1611.02997](#).
- [79] Y. Zheng, P. Hänggi, and D. Poletti, “Occurrence of discontinuities in the performance of finite-time quantum Otto cycles,” *Phys. Rev. E* **94**, 012137 (2016).
- [80] A. Kossakowski, A. Frigerio, V. Gorini, and M. Verri, “Quantum detailed balance and KMS condition,” *Commun. math. Phys.* **57**, 97 (1977).
- [81] H. Spohn, “An algebraic condition for the approach to equilibrium of an open N-level system,” *Lett. Math. Phys.* **2**, 33 (1977).

Supplemental Material for Universal Coherence-Induced Power Losses of Quantum Heat Engines in Linear Response

I. BOUND ON COHERENT POWER

We prove that the coherent power P^c as defined in Eq. 11 obeys the bound stated in Eq. 16. To this end, it is instructive to introduce the scalar product [1]

$$\langle X, Y \rangle \equiv \int_0^\beta d\lambda \operatorname{tr} \{ X^\dagger e^{-\lambda H} Y e^{(\lambda-\beta)H} \} / \operatorname{tr} \{ e^{-\beta H} \} \quad (1)$$

for any X and Y drawn from the space of system operators \mathcal{L} . Furthermore, we define the super-operators

$$HX \equiv [H, X]/\hbar \quad \text{and} \quad \mathbf{L} \equiv iH + \mathbf{D}^\dagger, \quad (2)$$

which have two important properties following from the detailed balance relation, Eq. 9. First, both, H and \mathbf{D} are self-adjoint with respect to the inner product (1). It follows that $\mathbf{L}^\ddagger = -iH + \mathbf{D}^\dagger$, where the double dagger indicates the super-operator adjoint with respect to (1). Second, H and \mathbf{D}^\dagger commute. Therefore, \mathbf{L} is normal, i.e., $\mathbf{L}\mathbf{L}^\ddagger = \mathbf{L}^\ddagger\mathbf{L}$ [2].

Using the definitions (1) and (2), Eq. 11 can be rewritten as

$$P^c = -\frac{1}{\mathcal{T}} \int_0^\mathcal{T} dt \int_0^\infty d\tau \dot{f}_t^w f_{t-\tau}^w \langle \mathbf{L} e^{\mathbf{L}\tau} \delta G^c, \delta G^c \rangle, \quad (3)$$

where

$$\delta X \equiv X - \langle 1, X \rangle / \beta \quad (4)$$

for any $X \in \mathcal{L}$. Due to its convolution-type structure, this expression is conveniently analyzed in Fourier space. Specifically, inserting the series

$$f_t^w \equiv \sum_{n \in \mathbb{Z}} c_n^w e^{in\Omega t} \quad (\Omega \equiv 2\pi/\mathcal{T}) \quad (5)$$

into (3) yields the mode expansion

$$P^c = \sum_{n \in \mathbb{Z}} P_n^c c_n^w c_n^{w*} = \sum_{n > 0} (P_n^c + P_n^{c*}) c_n^w c_n^{w*} \quad \text{with} \quad (6)$$

$$P_n^c \equiv \left\langle \frac{in\Omega \mathbf{L}}{in\Omega - \mathbf{L}} \delta G^c, \delta G^c \right\rangle,$$

$c_n^w = c_{-n}^{w*} \in \mathbb{C}$ and $c_0^w = 0$, since the period average of f_t^w vanishes by assumption. The second expression is thereby obtained by formally carrying out the improper integral in (3). This operation is well-defined, since the super-operator \mathbf{D}^\dagger is negative semidefinite, i.e., the eigenvalues of \mathbf{L} have non-positive real part [3].

The real part of the coefficient P_n^c defined in (6) can be bounded from above as follows. First, for $\mu \in \mathbb{R}$ and $n \neq 0$, we define the quadratic form

$$Q_n^c(\mu) \equiv \langle \mathbf{T}_n^{c+}(\mu) \delta G^c, (\mathbf{L} + \mathbf{L}^\ddagger) \mathbf{T}_n^{c+}(\mu) \delta G^c \rangle$$

$$+ \langle \mathbf{T}_n^{c-}(\mu) \delta G^c, (\mathbf{L} + \mathbf{L}^\ddagger) \mathbf{T}_n^{c-}(\mu) \delta G^c \rangle \leq 0 \quad \text{with}$$

$$\mathbf{T}_n^{c\pm}(\mu) \equiv \mp \mu \frac{\mathbf{L}^\ddagger \mp in\Omega}{in\Omega} \pm \frac{in\Omega}{\mathbf{L} \pm in\Omega}. \quad (7)$$

Note that $Q_n^c(\mu) \leq 0$, since the super-operator $\mathbf{L} + \mathbf{L}^\ddagger = 2\mathbf{D}^\dagger$ is negative semidefinite [3]. Second, we observe that

$$\langle Y^\dagger, Z^\dagger \rangle = \langle Y, Z \rangle^* = \langle Z, Y \rangle \quad \text{and} \quad (8)$$

$$(\mathbf{L}Y)^\dagger = \mathbf{L}Y^\dagger, \quad (\mathbf{L}^\ddagger Y)^\dagger = \mathbf{L}^\ddagger Y^\dagger \quad (9)$$

for arbitrary operators $X, Y \in \mathcal{L}$. Using these relations and the fact that the operator δG^c is Hermitian, the quadratic form (7) can be expanded as

$$Q_n^c(\mu) = 4\mu^2 \langle \mathbf{L} \delta G^c, \mathbf{L}^2 \delta G^c \rangle / (n\Omega)^2 + 4\mu^2 \langle \delta G^c, \mathbf{L} \delta G^c \rangle + 8\mu \langle \delta G^c, \mathbf{L} \delta G^c \rangle + 2(P_n^c + P_n^{c*}) \leq 0. \quad (10)$$

Maximizing this expression with respect to μ yields

$$P_n^c + P_n^{c*} \leq \frac{2 \langle \mathbf{L} \delta G^c, \delta G^c \rangle^2}{\langle \mathbf{L} \delta G^c, \delta G^c \rangle + \langle \mathbf{L} \delta G^c, \mathbf{L}^2 \delta G^c \rangle / (n\Omega)^2}$$

$$\leq \frac{2 \langle \mathbf{L} \delta G^c, \delta G^c \rangle^2}{\langle \mathbf{L} \delta G^c, \delta G^c \rangle + \langle \mathbf{L} \delta G^c, \mathbf{L}^2 \delta G^c \rangle / \Omega^2} \leq 0. \quad (11)$$

We now observe that

$$-\langle \mathbf{L} \delta G^c, \delta G^c \rangle = \int_0^\infty dt \langle e^{\mathbf{L}t} \mathbf{L} \delta G^c, \mathbf{L} \delta G^c \rangle$$

$$= \int_0^\infty dt \langle \hat{G}_t^{c(1)}, \hat{G}_0^{c(1)} \rangle = L_1^c \geq 0. \quad (12)$$

and

$$-\langle \mathbf{L} \delta G^c, \mathbf{L}^2 \delta G^c \rangle = \int_0^\infty dt \langle e^{\mathbf{L}t} \mathbf{L}^2 \delta G^c, \mathbf{L}^2 \delta G^c \rangle$$

$$= \int_0^\infty dt \langle \hat{G}_t^{c(2)}, \hat{G}_0^{c(2)} \rangle = L_2^c \geq 0. \quad (13)$$

Hence, the bound (11) can be cast into the compact form

$$P_n^c + P_n^{c*} \leq -\frac{2L_1^c \Omega^2}{\Omega^2 + L_2^c / L_1^c}. \quad (14)$$

Using this result to bound the mode expansion (6) yields

$$P^c \leq -\frac{2L_1^c \Omega^2}{\Omega^2 + L_2^c / L_1^c} \sum_{n > 0} c_n^w c_n^{w*}$$

$$= -\frac{L_1^c \Omega^2}{\Omega^2 + L_2^c / L_1^c} \frac{1}{\mathcal{T}} \int_0^\mathcal{T} dt (f_t^w)^2 \leq 0, \quad (15)$$

i.e., the upper bound stated in Eq. 16.

We note that, first, for $\Omega \rightarrow 0$, the coefficients P_n^c defined in (6) vanish such that $P^c \rightarrow 0$. Second, (7) and (10) imply

$$\lim_{\Omega \rightarrow \infty} Q_n^c(\mu = 0) = -4L_1^c = 2(P_n^c + P_n^{c*}). \quad (16)$$

Recalling (6), we thus obtain

$$\lim_{\Omega \rightarrow \infty} P^c = -2L_1^c \sum_{n>0} c_n^w c_n^{w*} = -\frac{L_1^c}{\mathcal{T}} \int_0^{\mathcal{T}} dt (f_t^w)^2. \quad (17)$$

Consequently, the bound (15) is saturated in the two limits $\Omega \rightarrow 0$ and $\Omega \rightarrow \infty$. Finally, the coefficients L_j^c defined in (12) and (13) vanish if and only if $\delta G^c = 0$, because all eigenvalues of \mathbf{L} have non-positive real part and the operator δG^c is orthogonal to the null space of \mathbf{L} . Since the set of Lindblad-operators $\{V_\sigma\}$ is self-adjoint and irreducible, this space contains only scalar multiples of the identity operator [3].

II. BOUND ON TOTAL POWER

The upper bound on the total power output stated in Eq. 19 can be established in two major steps. First, we observe that using Eq. 11 and the notation introduced in the previous section, $P = P^c + P^d$ can be written as

$$P = -\frac{1}{\mathcal{T}} \int_0^{\mathcal{T}} dt \int_0^{\infty} d\tau \left(\dot{f}_t^w f_{t-\tau}^w \langle \mathbf{L} e^{\mathbf{L}\tau} \delta G^c, \delta G^c \rangle + \dot{f}_t^w f_{t-\tau}^w \langle \mathbf{L} e^{\mathbf{L}\tau} \delta G^d, \delta G^d \rangle + \dot{f}_t^w f_{t-\tau}^q \langle \mathbf{L} e^{\mathbf{L}\tau} \delta G^d, \delta G^q \rangle \right). \quad (18)$$

Upon insertion of the Fourier series expansion

$$f_t^a \equiv \sum_{n \in \mathbb{Z}} c_n^a e^{in\Omega t} \quad (\Omega \equiv 2\pi/\mathcal{T}) \quad (19)$$

with $c_n^a = c_{-n}^{a*} \in \mathbb{C}$ and $a = w, q$, this expression becomes

$$P = \sum_{n \in \mathbb{Z}} (P_n^d + P_n^c) c_n^w c_n^{w*} + P_n^q c_n^w c_n^{q*} + \sum_{n>0} \left(1 + \frac{P_n^c + P_n^{c*}}{P_n^d + P_n^{d*}} \right) (P_n^d + P_n^{d*}) c_n^w c_n^{w*} + P_n^q c_n^w c_n^{q*} + P_n^{q*} c_n^{w*} c_n^q, \quad (20)$$

where

$$P_n^d \equiv \left\langle \frac{in\Omega \mathbf{L}}{in\Omega - \mathbf{L}} \delta G^d, \delta G^d \right\rangle = \left\langle \frac{in\Omega \mathbf{D}^\dagger}{in\Omega - \mathbf{D}^\dagger} \delta G^d, \delta G^d \right\rangle, \quad (21)$$

$$P_n^q \equiv \left\langle \frac{in\Omega \mathbf{L}}{in\Omega - \mathbf{L}} \delta G^d, \delta G^q \right\rangle = \left\langle \frac{in\Omega \mathbf{D}^\dagger}{in\Omega - \mathbf{D}^\dagger} \delta G^d, \delta G^q \right\rangle \quad (22)$$

and P_n^c was defined in (6). In (21) and (22), we could replace $\mathbf{L} = i\mathbf{H} + \mathbf{D}^\dagger$ by \mathbf{D}^\dagger since, by construction, both δG^d and δG^q commute with H , i.e., $\mathbf{H} \delta G^d = \mathbf{H} \delta G^q = 0$. We now observe that the real part of the coefficient P_n^d obeys

$$-2L_1^d \leq P_n^d + P_n^{d*} \leq 0, \quad (23)$$

where, analogous to (12),

$$L_1^d \equiv \int_0^{\infty} dt \langle \hat{G}_t^{d(1)}, \hat{G}_0^{d(1)} \rangle \geq 0. \quad (24)$$

This constraint can be derived by repeating the steps (7) to (14) with the quadratic from

$$Q_n^d(\mu) \equiv \langle \mathbf{T}_n^d(\mu) \delta G^d, \mathbf{D}^\dagger \mathbf{T}_n^d(\mu) \delta G^d \rangle \leq 0, \quad \text{where} \quad \mathbf{T}_n^d(\mu) \equiv \mu + \frac{in\Omega}{\mathbf{D}^\dagger + in\Omega} \quad \text{and} \quad n \neq 0, \mu \in \mathbb{R}. \quad (25)$$

With (14), (23) implies

$$1 + \frac{P_n^c + P_n^{c*}}{P_n^d + P_n^{d*}} \geq 1 + \frac{(L_1^c/L_1^d)\Omega^2}{\Omega^2 + L_2^c/L_1^c} \equiv \phi_\Omega \geq 1 \quad (26)$$

and thus, recalling (20),

$$P \leq \sum_{n>0} \phi_\Omega (P_n^d + P_n^{d*}) c_n^w c_n^{w*} + P_n^q c_n^w c_n^{q*} + P_n^{q*} c_n^{w*} c_n^q. \quad (27)$$

For the second step of our analysis, we note that the inequality (27) can then be rewritten as

$$P \leq \sum_{n>0} \phi_\Omega \left\langle \frac{in\Omega \mathbf{D}^\dagger}{in\Omega - \mathbf{D}^\dagger} \delta G^d + \frac{in\Omega \mathbf{D}^\dagger}{in\Omega + \mathbf{D}^\dagger} \delta G^d, \delta G^d \right\rangle c_n^w c_n^{w*} + \left\langle \frac{in\Omega \mathbf{D}^\dagger}{in\Omega - \mathbf{D}^\dagger} \delta G^d, \delta G^q \right\rangle c_n^w c_n^{q*} + \left\langle \frac{in\Omega \mathbf{D}^\dagger}{in\Omega + \mathbf{D}^\dagger} \delta G^d, \delta G^q \right\rangle c_n^{w*} c_n^q \quad (28)$$

$$= \sum_{n>0} 2\phi_\Omega \langle K_n, \mathbf{D}^\dagger K_n \rangle - \frac{\langle \delta G^q, \mathbf{D}^\dagger \delta G^q \rangle}{2\phi_\Omega} c_n^q c_n^{q*} \quad (29)$$

with

$$K_n \equiv c_n^w \frac{in\Omega}{\mathbf{D}^\dagger + in\Omega} \delta G^d + \frac{c_n^q}{2\phi_\Omega} \delta G^q. \quad (30)$$

Here, we have exploited that δG^d and δG^q are Hermitian operators, the relations (8) and (9) and the fact that the super-operator \mathbf{D}^\dagger is self-adjoint. Moreover, since, \mathbf{D}^\dagger is negative semidefinite, the first term under the sum in (29) is non-positive, while the second one is non-negative. Thus, we have

$$P \leq -\frac{\langle \delta G^q, \mathbf{D}^\dagger \delta G^q \rangle}{2\phi_\Omega} \sum_{n>0} c_n^q c_n^{q*} = -\frac{\langle \delta G^q, \mathbf{L} \delta G^q \rangle}{4\phi_\Omega} \frac{1}{\mathcal{T}} \int_0^{\mathcal{T}} dt (f_t^q - \bar{f}^q)^2. \quad (31)$$

Finally, making the identification

$$-\langle \delta G^q, \mathbf{L} \delta G^q \rangle = \int_0^{\infty} dt \langle \hat{G}_t^{q(1)}, \hat{G}_0^{q(1)} \rangle \equiv L_1^q \quad (32)$$

and defining $\psi_\Omega \equiv \phi_\Omega - 1$ completes our proof of Eq. 19.

III. OPTIMAL CLASSICAL DRIVING

We investigate the conditions that allow saturation of the quasi-classical bound on the total power output

stated in Eq. 21. To this end, using the previously introduced notation, the deviation of P from its upper limit $L_1^q F_q/4$ can be written in the form

$$P - L_1^q F_q/4 = 2 \sum_{n>0} \langle K'_n, D^\dagger K'_n \rangle \quad (33)$$

with

$$K'_n = c_n^w \frac{in\Omega}{D^\dagger + in\Omega} \delta G^w + \frac{c_n^q}{2} \delta G^q. \quad (34)$$

This expression can be obtained by repeating the derivation of (29) and invoking the additional condition $\delta G^c = 0$, which implies $\delta G^d = \delta G^w$.

From (33) and (34), it follows that $P = L_1^q F_q/4$ if and only if, each K'_n lies in the null space of the super-operator D^\dagger , i.e., if K'_n is a scalar multiple of the identity operator for any integer $n > 0$. This condition requires

$$0 = 2in\Omega c_n^w \delta G^w + in\Omega c_n^q \delta G^q + c_n^q D^\dagger \delta G^q. \quad (35)$$

We now observe that, since δG^w and δG^q must be Hermitian operators, (35) has a non-trivial solution only if

$$\delta G^w = \mu \delta G^q \quad \text{and} \quad D^\dagger \delta G^q = -\lambda \delta G^q \quad (36)$$

for some real μ and $\lambda > 0$, i.e., if the variable G^w is proportional to the unperturbed Hamiltonian H and δG^q is an eigenvector of D^\dagger . This connection can be established by splitting the Fourier coefficients c_n^w and c_n^q in real and imaginary parts and therewith separating (35) into two linear equations with real coefficients. Recalling the definition (4) and that $G_q = -H/T$, (36) can be written as

$$G^w = -\mu H/T \quad \text{and} \quad D^\dagger H = -\lambda(H - \langle H \rangle). \quad (37)$$

Provided the two conditions (36) are met, the solution of (35) reads

$$2in\Omega c_n^w = \lambda c_n^q/\mu - in\Omega c_n^q/\mu. \quad (38)$$

Inverting the Fourier transformation (19) thus yields the differential equation

$$2\dot{f}_t^w = \lambda(f_t^q - \bar{f}^q)/\mu - \dot{f}_t^q/\mu. \quad (39)$$

IV. SINGLE-QUBIT ENGINE

We consider the two-level engine described by the Hamiltonian shown in Eq. 26. For this system, the super-operator L defined in (2) has the explicit form

$$\begin{aligned} LX = & \frac{i\omega}{2} [\sigma_z, X] + \frac{\gamma e^\kappa}{2} (V_+[X, V_-] + [V_+, X]V_-) \\ & + \frac{\gamma e^{-\kappa}}{2} (V_-[X, V_+] + [V_-, X]V_+) \end{aligned} \quad (40)$$

with $V_\pm \equiv (\sigma_x \pm i\sigma_y)/2$. It fulfills

$$\begin{aligned} L\sigma_z &= -\lambda(\sigma_z + \tanh \kappa) = -\lambda(\sigma_z - \langle \sigma_z \rangle), \\ LV_\pm &= (\pm i\omega - \lambda/2) V_\pm. \end{aligned} \quad (41)$$

Using these relations and the fact that $\sigma_x = V_+ + V_-$, it is straightforward to evaluate the coefficients L_j^q defined in Eq. 18. Specifically, we find

$$\begin{aligned} L_j^c &= \frac{\hbar\omega\lambda(1-r)^2 \tanh \kappa}{4} (\omega^2 + \lambda^2/4)^{j-1}, \\ L_j^d &= \frac{\hbar\omega\lambda r^2 \kappa}{2 \cosh^2 \kappa} \lambda^{2(j-1)}, \\ L_j^q &= \frac{\hbar\omega\lambda \kappa}{2 \cosh^2 \kappa} \frac{\lambda^{2(j-1)}}{T^2}. \end{aligned} \quad (42)$$

Plugging these results into the general bounds given in Eqs. 16 and 19 yields Eq. 27.

For the plots of Fig. 2, we use the piecewise defined temperature profile

$$f_t^q = \Delta T \begin{cases} 1, & t \leq T/4 \\ 2 - 4t/T, & T/4 \leq t \leq T/2 \\ 0, & T/2 \leq t \leq 3T/4 \\ 4t/T - 3, & 3T/4 \leq t \leq T \end{cases} \quad (43)$$

with Fourier coefficients

$$c_0^q = \Delta T/2, \quad c_n^q = -\Delta T \frac{(-1)^n (i^n + 1)(i^n - 1)^2}{n^2 \pi^2} \quad (n \neq 0), \quad (44)$$

see (19). The Fourier coefficients of the work protocol defined through the conditions Eq. 28 and $\int_0^T dt f_t^w = 0$ are given by $c_0^w = 0$ and

$$c_n^w = \frac{1}{T} \frac{in - 1}{2in} c_n^q \quad (n \neq 0). \quad (45)$$

Evaluating the corresponding mean square amplitudes, which were defined in Eqs. 17 and 20, yields

$$\begin{aligned} F^w &= 2 \sum_{n>0} c_n^w c_n^{w*} = \frac{\Delta T^2}{T^2} \frac{\pi^2 + 10}{240} \quad \text{and} \\ F^q &= 2 \sum_{n>0} c_n^q c_n^{q*} = \frac{\Delta T^2}{6}. \end{aligned} \quad (46)$$

Furthermore, the mode expansion coefficients of the coherent and the classical power, which were introduced in (6), (21) and (22), respectively, become

$$\begin{aligned} P_n^c &= \frac{\hbar\omega(1-r)^2 \tanh \kappa}{4} \\ &\quad \times \left(\frac{in\Omega(i\omega - \lambda/2)}{in\Omega + (i\omega - \lambda/2)} - \frac{in\Omega(i\omega + \lambda/2)}{in\Omega - (i\omega + \lambda/2)} \right), \\ P_n^d &= \frac{\hbar\omega r^2 \kappa}{2 \cosh^2 \kappa} \frac{in\Omega\lambda}{\lambda - in\Omega}, \\ P_n^q &= -\frac{1}{T} \frac{\hbar\omega r \kappa}{2 \cosh^2 \kappa} \frac{in\Omega\lambda}{\lambda - in\Omega}. \end{aligned} \quad (47)$$

The plots shown in Fig. 2 are now obtained by numerically approximating the improper sums in (6) and (20).

-
- [1] R. Kubo, M. Toda, and N. Hashitsume, *Statistical Physics II - Nonequilibrium Statistical Mechanics*, 2nd ed. (Springer, Tokyo, 1998).
- [2] K. Brandner and U. Seifert, “Periodic thermodynamics of open quantum systems,” *Phys. Rev. E* **93**, 062134 (2016).
- [3] H. Spohn, “An algebraic condition for the approach to equilibrium of an open N-level system,” *Lett. Math. Phys.* **2**, 33 (1977).